ELSEVIER

Thermochimica Acta 277 (1996) 165–173

thermochimica acta

The use of master plots for discriminating the kinetic model of solid state reactions from a single constant-rate thermal analysis (CRTA) experiment

L.A. Pérez-Maqueda, A. Ortega, J.M. Criado *

Dpto de Química Inorgánica e Instituto de Ciencia de Materiales de Sevilla, Centro coordinado C.S.I.C.-Universidad de Sevilla, Sevilla, Spain

Received 29 March 1995; accepted 12 September 1995

Abstract

A new method has been outlined that improves the discrimination of the kinetic model fitted by a solid state reaction from a single CRTA experiment, by means of a series of master plots that represent the values of $(T_{0.5}/T)^2[d\alpha/dT)_{0.5}/(d\alpha/dT)]$ as a function of α. The suffix 0.5 refers to the values of the temperature T and $d\alpha/dT$ when the fraction reacted α is 0.5. Kinetic analyses of the thermal decompositions of calcium carbonate and anhydrous nickel nitrate have been used to check this method.

Keywords: CRTA; Kinetic model; Master plots; Solid state reaction

1. Introduction

It has been reported in previous papers [1–4] that the morphology, texture and structure of ceramic materials can be controlled by decomposing their corresponding precursors by means of constant-rate thermal analysis (CRTA).

However, it has been claimed [5–7] that CRTA reduces the influence of heat and mass transfer phenomena on the forward solid state reaction with regard to the conventional thermal methods. Moreover, it has been suggested that CRTA has a higher resolution power than conventional DTA–TG for separating overlapping processes [8, 9] and, at the same time, has a higher efficiency for discriminating the actual kinetic models obeyed by the reaction [10]. Thus, it has been claimed that CRTA

* Corresponding author.

SSDI 0040-6031(95)02746-7

shows numerous advantages over the conventional approach [11,12] which explains its recent commercialization by a number of manufacturers of thermobalances and dilatometers [13], including Netzch, Setaram, TA Instruments, etc.

The scope of the present paper is to devolop a series of master curves characteristic of the different kinetic models that depend neither on the kinetic parameters (activation energy and Arrhenius pre-exponential factor) nor on the reaction rate C selected for recording the CRTA experiment. We expect that this method will improve the analysis of kinetic data for solid state reactions.

2. Experimental

$Ni(NO_3)_2 \cdot 6H_2O$ (Panreac a.r.) and $CaCO_3$ (Aldrich a.r.) were used. The anhydrous nickel nitrate was prepared by dehydrating the hexahydrate in the crucible of the microbalance at 150°C under vacuum for three hours before starting the CRTA experiment.

A 2000 CAHN electrobalance attached to a high-vacuum system was used. The apparatus has been modified in order to monitor the furnace temperature in such a way that the total decomposition rate remains constant over the entire range. This has been attained both by controlling the residual pressure in the close vicinity of the sample and by maintaining a constant value of the pumping rate which can be selected by means of a high-vacuum value. The CRTA diagrams were obtained using a constant residual pressure of 10^{-4} mbar, and a decomposition rate of about 2.85×10^{-3}. A data logger (Linseis, model 18500) that allows a maximum frequency of aquisition data of 13 kHz with a resolution power of 16 bit was used for collecting the values of the reacted fraction α as a function of T. The corresponding $d\alpha/dT$ values were determined by means of the differentiate utility included in the Microcal Origin program for PC computers (Microcal Software, Inc.).

3. Theoretical

Bearing in mind that CRTA diagrams are obtained at a constant rate $C = d\alpha/dt$, and taking into account the general expression of the reaction rate, we can write

$$C = A f(\alpha) \exp(-E/RT) \tag{1}$$

where α is the reacted fraction at the time t, $f(\alpha)$ is a function depending on the reaction mechanism (Table 1) and other symbols have their usual meaning.

Taking derivatives of Eq.(1), we get

$$\frac{dT}{dt}\frac{1}{T^2} = -\frac{RC}{E}\frac{f'(\alpha)}{f}(\alpha) \tag{2}$$

For temperature $T_{0.5}$, which corresponds to $\alpha = 0.5$, we get

$$\left(\frac{dT}{dt}\right)_{0.5}\frac{1}{T_{0.5}} = -\frac{RC}{E}\frac{f'(0.5)}{f(0.5)} \tag{3}$$

From Eq. (2) and (3) we get

$$\frac{(dT/dt)}{(dT/dt)_{0.5}}\left(\frac{T_{0.5}}{T}\right)^2 = \frac{f'(\alpha)}{f(\alpha)}a \tag{4}$$

Taking into account that $C = d\alpha/dt$, Eq. (1) can be rearranged in the form

$$\frac{(d\alpha/dT)_{0.5}}{(d\alpha/dT)}\left(\frac{T_{0.5}}{T}\right)^2 = a\frac{f'(\alpha)}{f(\alpha)} \tag{5}$$

where $a = f(0.5)/f'(0.5)$ is a constant for a given mechanism, and $(d\alpha/dT)_{0.5}/(d\alpha/dT)$ is defined here after as the reduced rate. Table 1 shows the values for the constant a and the $f(\alpha)$ and $f'(\alpha)$ functions for the kinetic models more commonly used in the literature for describing solid state reactions.

Eq. (5) indicates that a plot of the left-hand-side of the equation α depends neither on the kinetic parameters nor on the reaction rate C, but only on the reaction mechanism. Fig. 1 shows a series of master curves calculated for the different kinetic models included in Table 1. We can see that just by looking at the shape of these plots one can easily discriminate between the three following families of kinetic models: phase

Table 1
The $f(\alpha)$ and $f'(\alpha)$ functions and the a constant for the most common kinetic models used in the literature

Mech.	$f(\alpha)$	$f'(\alpha)$	a
R2	$(1-\alpha)^{1/2}$	$\frac{-1}{2(1-\alpha)^{1/2}}$	-1
R3	$(1-\alpha)^{2/3}$	$\frac{-2}{3(1-\alpha)^{1/3}}$	$-3/4$
F1	$(1-\alpha)$	-1	$-1/2$
A2	$2(-\ln(1-\alpha))^{1/2}(1-\alpha)$	$\frac{2\ln(1-\alpha)+1}{[-\ln(1-\alpha)]^{1/2}}$	-1.7943
A3	$3(-\ln(1-\alpha))^{2/3}(1-\alpha)$	$\frac{3\ln(1-\alpha)+2}{[-\ln(1-\alpha)]^{1/3}}$	-13.0879
D2	$\frac{-1}{\ln(1-\alpha)}$	$\frac{-1}{[\ln(1-\alpha)]^2(1-\alpha)}$	-0.3466
D3	$\frac{3(1-\alpha)^{2/3}}{2[1-(1-\alpha)^{1/3}]}$	$\frac{1/2-(1-\alpha)^{-1/3}}{[1-(1-\alpha)^{1/3}]^2}$	-0.2565
D4	$\frac{3}{2[(1-\alpha)^{-1/3}-1]}$	$\frac{-1}{2[(1-\alpha)^{1/3}-1]^2(1-\alpha)^{2/3}}$	-0.3094

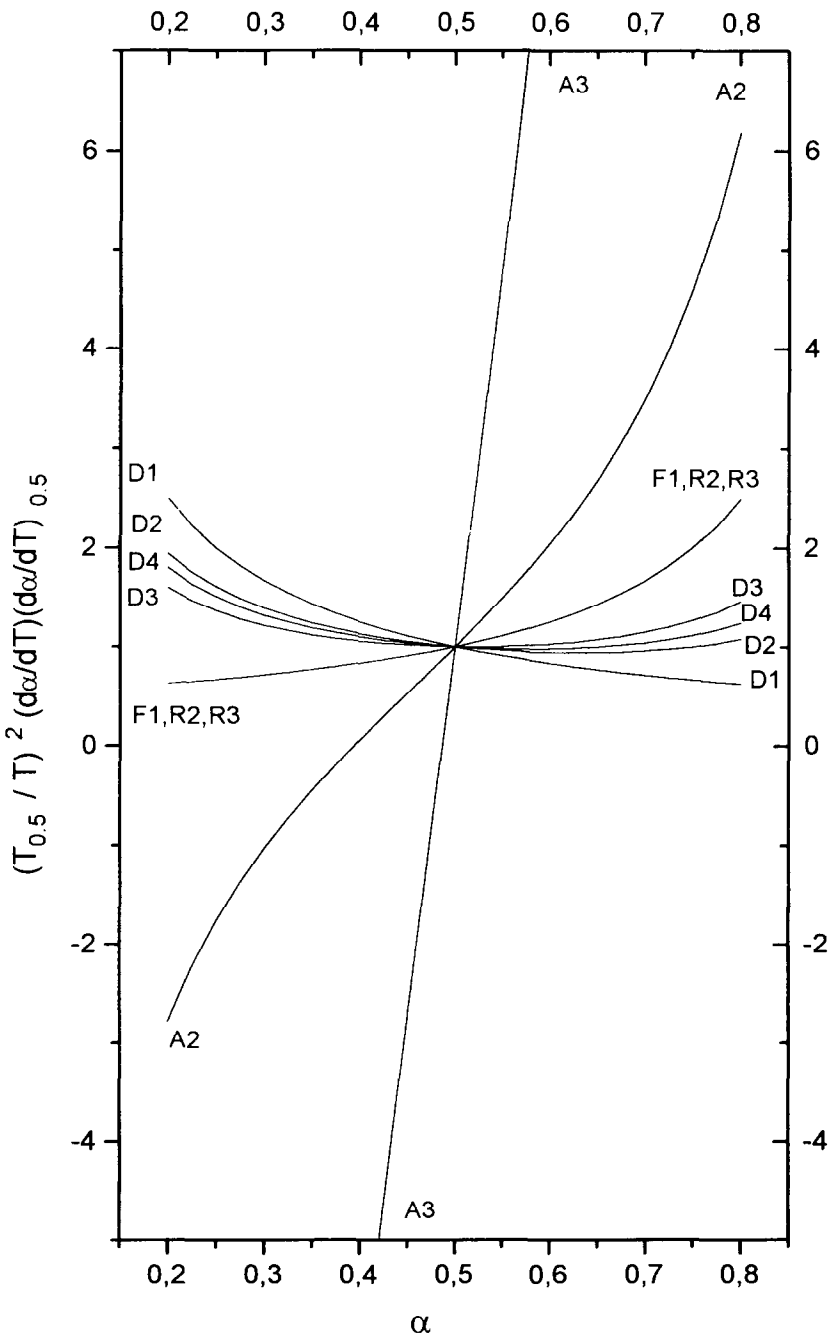

Fig. 1. Theoretical master curves representing the "reduced rate" calculated from CRTA traces as a function of α for the different kinetic models describing solid state reactions.

boundary (n-order kinetic), nucleation and growth of nuclei (Avrami–Erofeev), and diffusion-controlled reactions. Moreover, the high resolution power of this method for discriminating among the different Avrami–Erofeev kinetic laws should be noted.

4. Results

The kinetics of the thermal decomposition of $CaCO_3$ and anhydrous nickel nitrate has been analysed in previous papers [14,15] for both isothermal and conventional TG experiments. It was concluded that the decarbonation of $CaCO_3$ under high vacuum fitted an R_3 (contracting sphere) kinetic model with an activation energy of 179 kJ/mol^{-1} [14]. However, it was reported [15] from TG data associated with mass

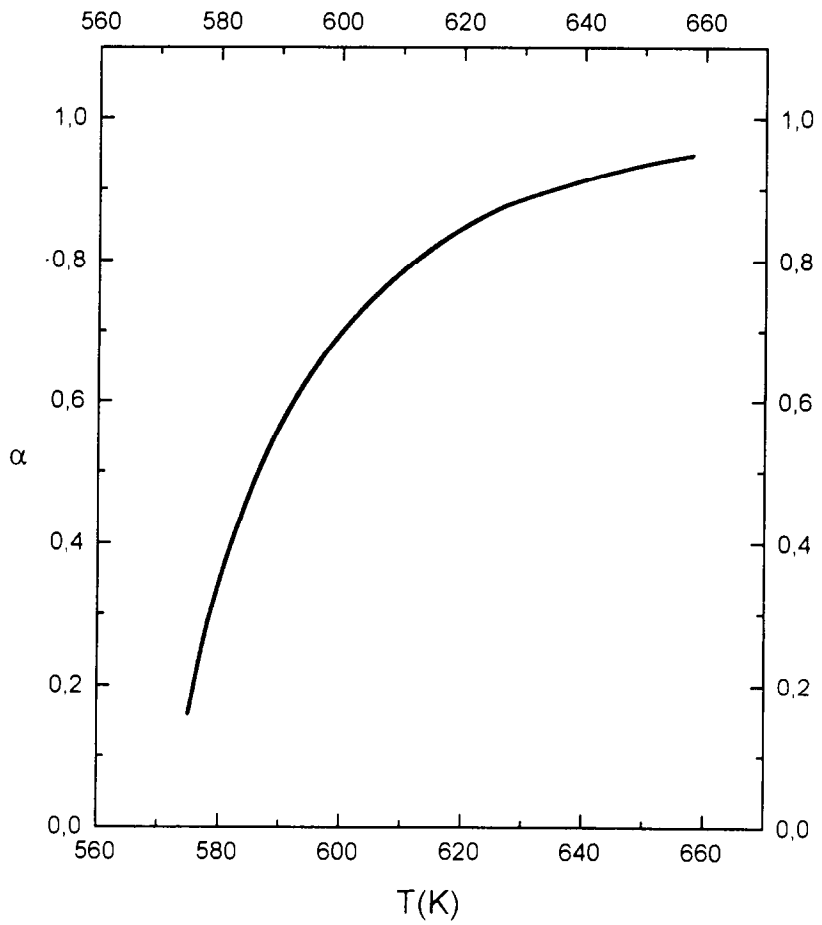

Fig. 2. CRTA curve of thermal decomposition of $CaCO_3$ recorded at a constant rate $c = 2.85 \times 10^{-3}$ min^{-1} under a vacuum of 10^{-4} mbar.

spectrometry experiments that the thermal decomposition of nickel nitrate takes place through a single step, represented by the equation

$$Ni(NO_3)_2 \rightarrow NiO + 2NO_2 + 1/2O_2 \quad (6)$$

It was concluded that this reactions fits an A_2 Avrami–Erofeev kinetic model with an activation energy $E = 684$ kJ mol^{-1}.

Taking into account the above considerations, the themal decompositions of $CaCO_3$ and $Ni(NO_3)$ are suitable for checking the master plots included in Fig. 1. Thus, the same samples of these materials studied by us in Refs. [14] and [15] were used here. Fig. 2 shows the CRTA curves recorded for the thermal decomposition of $CaCO_3$; the CRTA trace obtained for the thermal decomposition of anhydrous nickel nitrate is shown in Fig. 3.

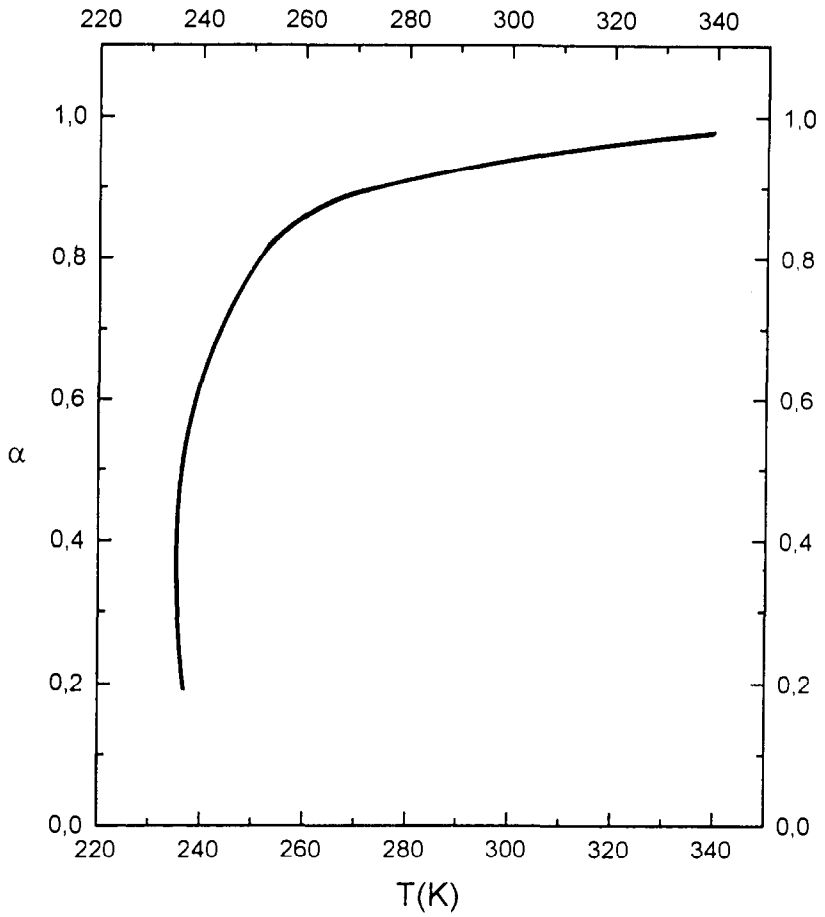

Fig. 3. CRTA trace obtained for the thermal decomposition of anhydrous nickel nitrate at a constant rate $c = 2.85 \times 10^{-3}$ min^{-1} under a vacuum of 10^{-4} mbar.

The values of the left-hand-side of Eq. (5) calculated from the data included in Figs. 2 and 3 are plotted as a function of α in Figs. 4 and 5 respectively. The experimental reduced rate plots obtained for the thermal decomposition of $CaCO_3$ and $Ni(NO_3)_2$ are compared in Figs. 4 and 5 with the master plots corresponding to the R_3 and A_2

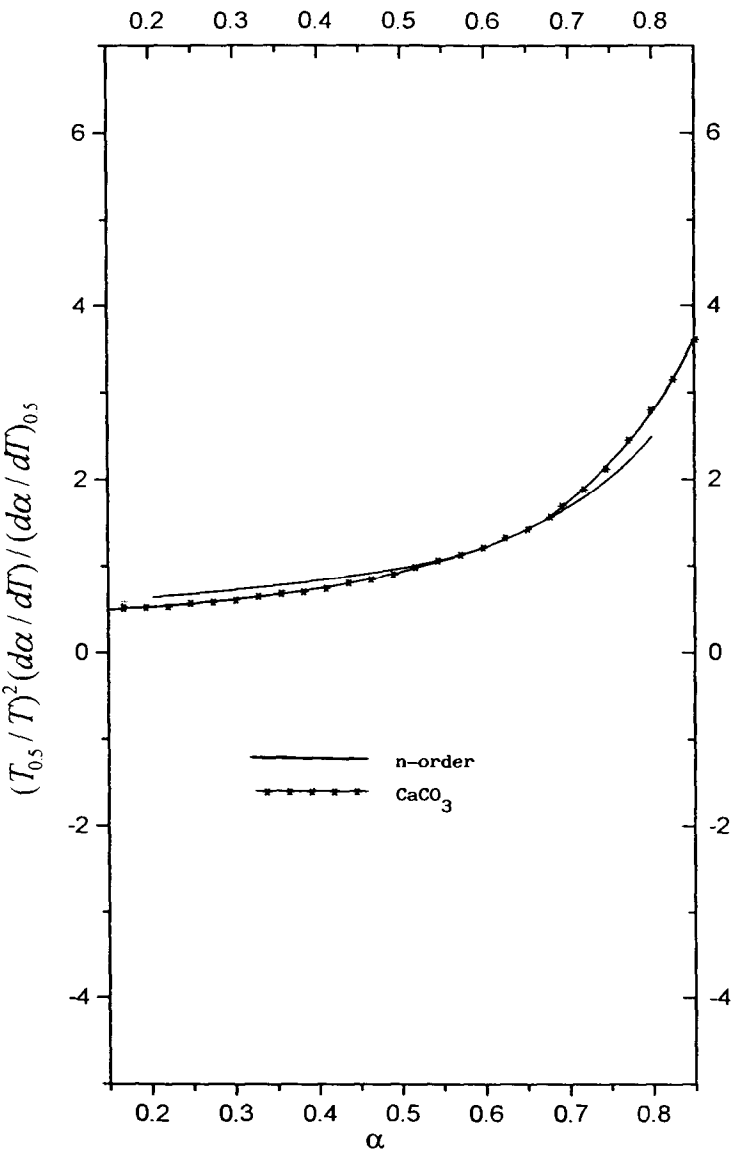

Fig. 4. A comparison of the experimental "reduced rate" plot of the thermal decomposition of $CaCO_3$ with the corresponding master curve representing "*n*-order" kinetic models.

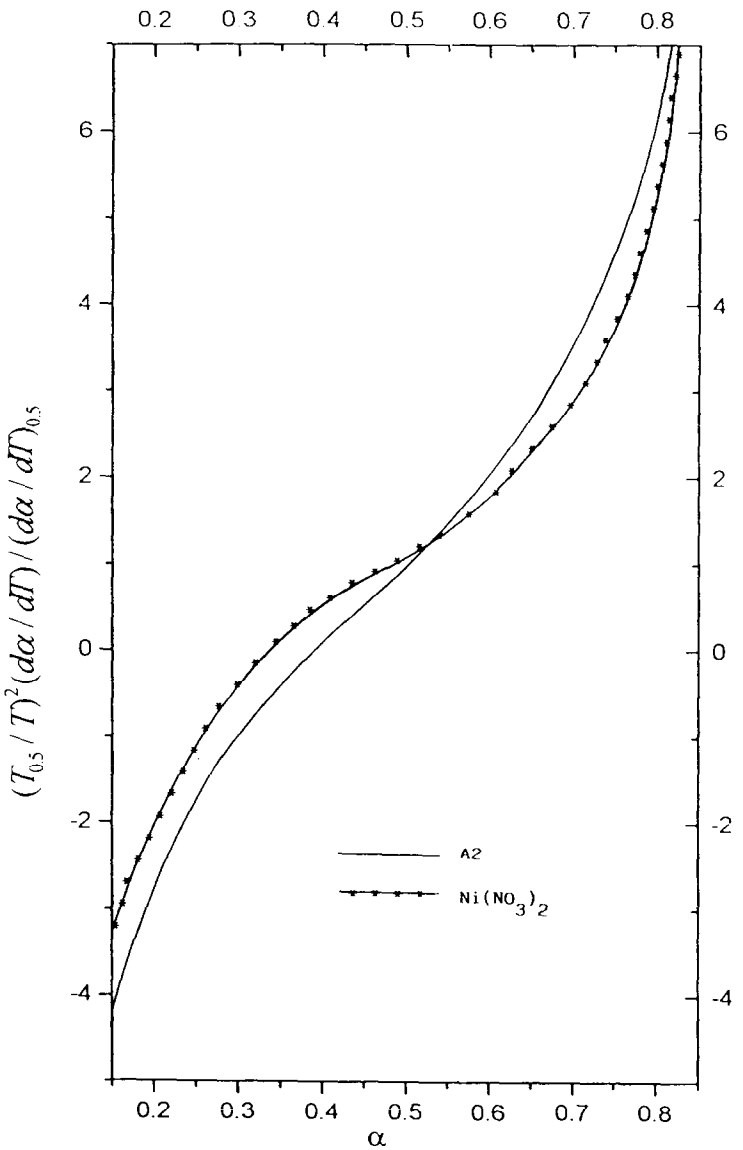

Fig. 5. A comparison of the experimental "reduced rate" curve of the thermal decomposition of anhydrous nickel nitrate with the master curve corresponding to an A_2 model.

kinetic models, respectively. The good fit of the experimental data of the theoretical master curves corresponding to the kinetic laws obeyed by the above reactions according to the results reported in previous papers is apparent.

In summary, we conclude that the method outlined allows a quick selection of the actual kinetic rate expression obeyed by a solid state reaction, unless an "*n*-order"

kinetic model is fitted. In such a case it would be determined with greater accuracy that an "*n*-order" reaction alone without the use of additional information in deciding the value of *n*. These results are in agreement with those reported in previous papers where it was concluded that is not possible to determine at the same time the "*n*-order" and activation energy of a solid state reaction from a single CRTA experiment.

Reference

[1] J. Rouquerol, M. Ganteaume. J. Therm. Anal., 11 (1977) 201.
[2] J.L. Garcia-Fierro. React. Solids, 1 (1985) 103.
[3] J.M. Criado, F.J. Gotor, C. Real, F. Jimenez, S. Ramos and J. Del Cerro, Ferroelectrics, 115 (1991) 43.
[4] A. Dwivedi and R.F. Speyer, Thermochim. Acta, 247 (1994) 431.
[5] J.M. Criado, F. Rouquerol and J. Rouquerol. Thermochim. Acta, 38 (1980) 109.
[6] A. Ortega, S. Akhouyasi, F. Rouquerol and J. Rouquerol, Thermochim. Acta, 235 (1994) 197.
[7] J.M. Criado, A. Ortega and J. Rouquerol, Bol. Soc. Esp. Ceram. Vid., 26 (1987) 3.
[8] J. Paulik and F. Paulik, Simultaneous thermoanalytical examinations by means of the derivatograph, in Comprehensive Analytical Chemistry, Vol. XII, Part A, Elsevier, Amsterdam, 1981, p. 14.
[9] F. Paulik and J. Paulik, Thermochim. Acta, 100 (1986) 23.
[10] J.M. Criado, A. Ortega and F. Gotor, Thermochim. Acta, 157 (1990) 171.
[11] M. Reading, Controlled Rate Thermal Analysis and Beyond, in E.L. Charsley and Warrington (Eds.), Thermal Analysis—Techniques and Applications, The Royal Society of Chemistry, London, 1992.
[12] J. Rouquerol, Thermochim. Acta, 144 (1989) 209.
[13] P.S. Gill, S.R. Sauerbrunn and B.S. Crowe, J. Therm. Anal., 38 (1992) 255.
[14] J.M. Criado, M. Gonalez, A. Ortega and C. Real, J. Therm. Anal., 29 (1984) 243.
[15] J.M. Criado, A. Ortega and C. Real, React. Solids, 4 (1987) 93.